Hindawi
Geofluids
Volume 2020, Article ID 8879477, 16 pages
https://doi.org/10.1155/2020/8879477

Research Article

Investigation of Burn Cut Parameters and Model for One-Step Raise Excavation Based on Damage Evolution Mechanisms

Kai Liu[1] **and Jiadong Qiu**[2,3]

[1]*School of Civil Engineering, Guangzhou University, Guangzhou Guangdong 510006, China*
[2]*Key Laboratory of Metallogenic Prediction of Nonferrous Metals and Geological Environment Monitoring (Central South University), Ministry of Education, China*
[3]*Shenzhen Key Laboratory of Deep Underground Engineering Sciences and Green Energy, Shenzhen University, Shenzhen 518060, China*

Correspondence should be addressed to Jiadong Qiu; jdq1991@csu.edu.cn

Received 11 September 2020; Revised 14 October 2020; Accepted 2 November 2020; Published 24 November 2020

Academic Editor: Yanlin Zhao

One-step raise excavation with burn cut is a kind of technology which use the drilling and blasting method to excavate the raise quickly. Due to the limitation of the free surface in burn cut, determination of cut parameters such as the length of burden and diameters of empty hole and charge hole is important to achieve a good effect of cut blasting. Meanwhile, the choice of the cut model is also crucial to form a proper opening. In this study, a modified Holmquist-Johnson-Cook (HJC) model, in which the tension-compression damage model and tension-compression strain rate effect model are considered, is embedded in the LS-DYNA software to investigate the damage evolution of rock in cut blasting. A simplified numerical model of burn cut is built in the LS-DYNA. The numerical results indicate that there is a threshold value of the burden length to maximize the opening. The empty hole has the effect of transferring blasting energy, and the effect becomes more obvious with the increase of the hole size. Moreover, the linear charge density of the prime cut hole can affect the compression and tension damage. Further, the comparison among four typical burn cut models are conducted based on numerical results. It demonstrates that triangular prism cut and doliform cut, which have more empty holes arrangement surrounding the prime cut hole, are better than spiral cut and diamond cut that with less empty holes locating one side of the prime cut hole in terms of energy efficiency and damage zone control.

1. Introduction

Because of the advantages of high efficiency, simple operation, and low cost, the drilling and blasting method has always been the main method in rock excavation engineering such as mining, tunneling, and underground space development. Unlike bench blasting, in which burden rock is directed towards two or more free surfaces, there are only one free surface in tunnel and raise excavation blasting. Thus, cut blasting is the most critical step in the process of tunnel and raise excavation since it can create an opening as a second free surface for the subsequent borehole blasting. In the process of cut blasting, the prime cut hole takes the empty holes as the free surface and swelling space, so the corresponding burden rock is subjected to high degree of constriction [1]. The opening created by the prime cut hole is determined by cut parameters such as burden length and size of empty hole and prime cut hole [2]. In order to obtain a good cut blasting effect, it is crucial to investigate the damage evolution mechanisms of the burden rock of the prime cut hole blasting under different cut parameters.

For the study of rock blasting, numerical simulation is more efficient and flexible compared with the theoretical derivation and field test. Therefore, numerical simulation has become the main technique to investigate the damage evolution mechanisms of rock blasting [3–7]. In order to simulate damage evolution of brittle materials such as rock and concrete under dynamic load, many classical damage

models, such as the Taylor–Chen–Kuszmaul (TCK) model [8], Holmquist–Johnson–Cook (HJC) model [9], and Riedel–Hiermaier–Thoma (RHT) model [10], were proposed and developed. To predict the size and shape of the blasting crater in rock mass, the TCK model was used to study the dynamic fracture behavior of rock in tension by Wang et al. [11]. Fang et al. [12] determined the parameters of the HJC model for rock and then used it to simulate the projectile penetration test of granite. Liu et al. [13] used the RHT model to simulate the damage evolution process of cut blasting. The cut parameters were optimized based on numerical results and verified by field tests. However, these models have some inherent drawbacks, for example, the TCK model only considers the tension damage [14]. In contrast, the HJC model only takes the compression damage into account [15, 16]. In the RHT model, many material parameters, which are complicated and difficult to be obtained by experiments, should be determined [17]. In order to more truly reflect the dynamic response and failure characteristic of rock under impact load, researchers have proposed many new models or improved the existing models [18–20]. Liu and Katsabanis [21] introduced a continuum damage model, which was calibrated by field crater blasting and small bench blasting tests, to study the damage zone distribution under different loading rates and rock stiffness. Tu and Lu [22] implemented an improved RHT model into the AUTODY, and then the improved RHT model was used to simulate projectile penetration.

Although the damage evolution mechanisms of rock blasting have been studied by many researchers, little work has been conducted on the investigation of cut blasting. For this case, Xie and Lu [23] investigated the influence of in situ stress on damage evolution to rock mass under the Swedish cut model; further, a burden optimization was conducted for burn cut in the deep tunnel. However, the effect of other cut parameters was not considered. Taking the empty hole as an example, on one hand, the larger empty hole, the more vulnerable the burden rock is to breakage. On the other hand, the larger empty hole, the higher cost of drilling [24]. In addition, the determination of cut parameters will affect each other. For example, when the burden length is increased, the corresponding diameter of the empty hole should be increased to ensure there is enough swelling space for rock fragments. The relationship between them can be expressed by an indicator of the swelling ratio, which is defined as the volume of swelling space divided by the volume of the burden rock. Moreover, the design of the cut model also is an important step in the overall cut blasting procedure, because the layout of boreholes has important influence on the size of opening, the utilization of explosive energy, and the difficulty of drilling.

In the present paper, in order to study the influence of cut parameters that include the burden and the diameter of the empty hole and prime cut hole on rock damage evolution, a simplified cut numerical model is established in LS-DYNA. A tension-compression damage model, which is improved by the author based on the original HJC model, is implemented into LS-DYNA and employed for the rock material [25]. According to the analysis of the simulation results, the relationship between the cut parameters and damage evolution is revealed, and the optimal cut parameters are determined. Further, the optimal cut parameters are applied on four typical burn cut models, in which the comparison between the utilization of explosive energy and the damage evolution is made. In addition, it is necessary to note that the explosive energy is converted into two basic forms that are stress wave energy and gas energy when the explosive detonates [26]. Most of the stress wave energy is expended on the creation of the compression damage zone and radial crack zone; then, the cracks are further developed under the action of gas pressure. Nevertheless, only the damage evolution produced by stress wave is considered in the numerical simulation, and this simplification can give reasonable damage prediction in numerical simulation according to some previous researches [27–29]. Thus, the blasting damage induced by gas pressure is not considered in this study.

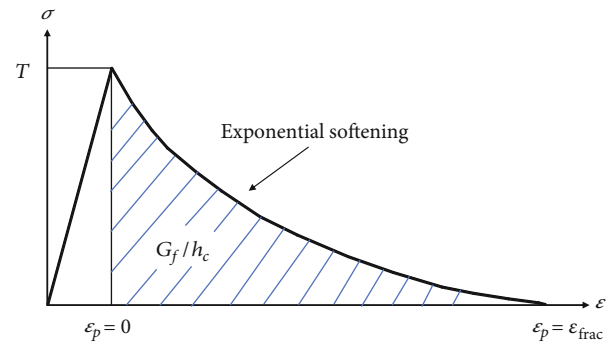

Figure 1: Exponential stress-strain curve for uniaxial tension.

2. Material Models

2.1. Tension-Compression Damage Model for Rock. In the damage evolution process of rock under blasting loading, the rock damage is affected by radial compressive stress, hoop tensile stress, and reflection tensile stress [30]. Therefore, rock damage induced by blasting load can be divided into compression damage and tension damage. Meanwhile, rock is more sensitive to tensile stress because of the lower tensile strength of rock [31–33]. Thus, rock mainly showed as tension damage and many tension cracks will appear result in rock fragmentation under dynamic load [34–37]. Thus, the accumulation of tension damage and compression damage should be considered separately.

In addition, the strain rate effect, which can enhance the dynamic strength of material, is a characteristic of rock under dynamic load [21, 38]. Under the action of dynamic load, the tensile strain rate effect appears to be more sensitive than the compressive strain rate effect. That means that at the same strain rate, the dynamic increase factor (DIF) produced by tensile stress is greater than that produced by compressive stress. Thus, the strain rate effect for tension and compression should be also calculated separately. In the previous

Table 1: Parameters of the modified HJC model.

ρ/(kg/m^3)	G/GPa	K/GPa	B	N	f_c/MPa	f_t/MPa	D_1	D_2
3471	32.09	46.6	2.51	0.64	173.1	8.72	0.04	1.0
p_c/MPa	μ_c	p_l/GPa	μ_l	K_1/GPa	K_2/GPa	K_3/GPa	EF_{min}	ε_{frac}
57.7	0.0012	1.92	0.100	17.8	9.9	104.1	0.01	0.0017

study, a modified HJC model, which considered the tension-compression damage and strain rate effect, was implemented into the LS-DYNA by the authors [25]. The modified HJC model can well reflect the rock mechanical performance under dynamic load; thus, it is applied in this study.

2.1.1. Strain Rate Effect Model. For brittle materials, the DIF induced by tensile load is higher than that induced by compressive load under the same strain rate. Therefore, the DIFs of tension and compression should be calculated, respectively, in the modified HJC model. Most of the strain rate effect models proposed by many researchers were exponential models [23]. However, according to the investigation of Qi and Qian [39], the curve of the DIF and strain rate shown a hyperbolic tangent shape. Therefore, a hyperbolic function [40], which could describe the strain rate effect of rock, was introduced in the modified HJC model.

$$\mathrm{DIF}_t = \left\{ \left[\tanh\left(\left(\lg\left(\frac{\dot{\varepsilon}}{\dot{\varepsilon}_0} \right) - W_x \right) S \right) \right] \left[\frac{F_m}{W_y} - 1 \right] + 1 \right\} W_y, \tag{1}$$

where DIF_t is the dynamic increase factor for tension. $\dot{\varepsilon}_0 = 1\mathrm{s}^{-1}$ is the reference strain rate. $W_x = 1.6$, $S = 0.8$, $F_m = 10$, and $W_y = 5.5$ are the fitting constants, which are determined based on the research of Tedesco et al. [41]. Further, the expression of the dynamic increase factor for compression (DIF_c) can be established under the assumption that the tensile increment is equal to the compressive increment at same strain rates.

$$\mathrm{DIF}_c = (\mathrm{DIF}_t - 1)\left(\frac{T}{f_c} \right) + 1, \tag{2}$$

where T is the maximum hydrostatic tension, and f_c is the quasistatic uniaxial compressive strength.

2.1.2. Damage Model. In the original HJC model, the damage is induced by the accumulation of the plastic strain and the plastic volume strain, which can well reflect the compressive damage of rock. Details of the damage model of the original HJC model can be found in Johnson and Holmquist [9]. The damage model in the original HJC model continues to be used as the compressive damage model in the modified HJC model.

Table 2: Parameters of explosive material and JWL EOS.

ρ_e (kg/m^3)	V_0D (m/s)	P_{CJ} (GPa)	A_J (GPa)	B_J (GPa)	R_1	R_2	ω	E_0 (GPa)
1210	5660	9.7	214.4	0.182	4.2	0.9	0.15	4.192

In the modified HJC model, the tension damage is described as an exponential softening model proposed by Weerheijm and Doormaal [42], as follows.

$$D_t = \left[1 + \left(c_1 \frac{\varepsilon_P}{\varepsilon_{frac}} \right)^3 \right] \exp\left(-c_2 \frac{\varepsilon_P}{\varepsilon_{frac}} \right) - \frac{\varepsilon_P}{\varepsilon_{frac}} \left(1 + c_1^3 \right) \exp\left(-c_2 \right), \tag{3}$$

where $\varepsilon_P = \sum \Delta\varepsilon_p$ is the effective plastic strain, and ε_{frac} is the fracture strain which is depended on element size in the numerical model. The constants are $c_1 = 3$ and $c_2 = 6.93$.

For the exponential softening model, the stress-strain curve of uniaxial tension is shown in Figure 1. The strain energy can be obtained by the given fracture energy during the entire tensile cracking process of the element, as follows.

$$\int_{\varepsilon_p=0}^{\varepsilon_p=\varepsilon_{frac}} \sigma d\varepsilon = \frac{G_f}{h_c}, \tag{4}$$

where G_f is the fracture energy, and h_c is the characteristic length of the element which can be approximated as the cube root of the volume of the element in a 3-D numerical model. Besides, in order to show the presidential damage during rock failure, the final damage variable is determined by

$$D = \mathrm{Max}\left(D_c, D_t \right). \tag{5}$$

In order to avoid the discontinuity of the yield surface at the point of $p = 0$, an improved yield function is proposed by Polanco-Loria et al. [15]. Meanwhile, the Lode-angle function $R(\theta)$ is introduced to describe the shape change of the yield surface on the deviatoric plane.

$$\sigma^* = \begin{cases} \mathrm{B}[T^*(1-\mathrm{D}) + p^*]^N \mathrm{R}(\theta, e)\mathrm{DIF}, \mathrm{P}^* \geq -\mathrm{T}^*(1-\mathrm{D}) \\ 0 \mathrm{P}^* < -\mathrm{T}^*(1-\mathrm{D}) \end{cases} \tag{6}$$

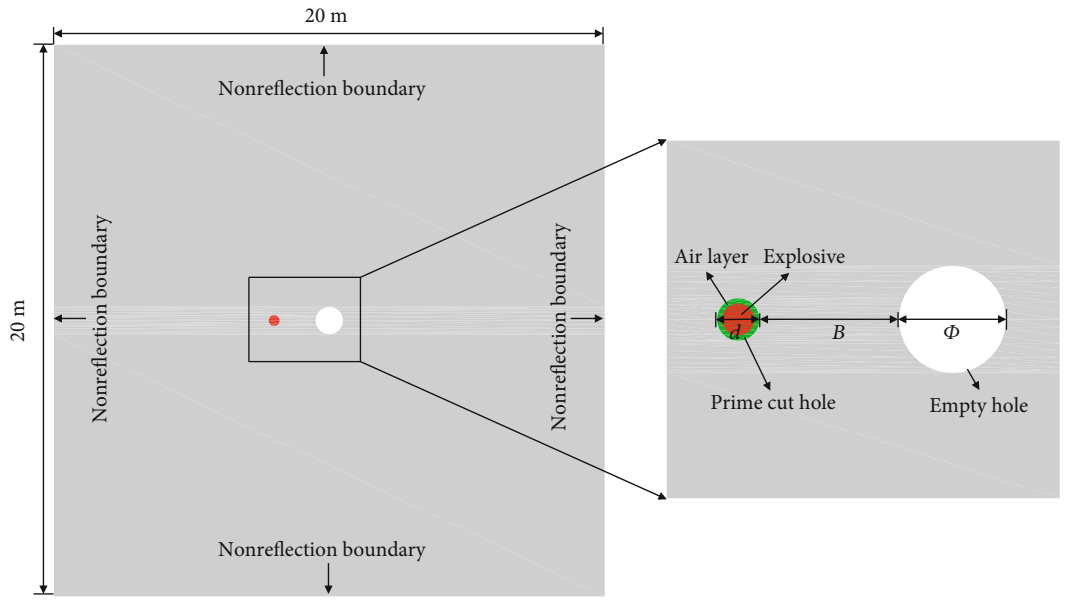

Figure 2: Prime cut blasting numerical model geometry and boundary conditions.

where $\sigma^* = \sigma/f_c$ and $T^* = T/f_c$ are the normalized equivalent stress and the normalized hydrostatic tension, respectively. $p^* = p/f_c$ denotes the normalized pressure, where p is the actual pressure. B and N are the material constants. In this study, the engineering background is consistent with the rock blasting test in Liu et al. [25]. So, the basic rock mechanical parameters are also consistent with Ref. [25]. However, considering the high degree of constriction in burn cut, the rock mechanical parameters are not reduced. According to the method in Ref. [25], the parameters of modified HJC are obtained and shown in Table 1.

2.2. Jones-Wilkins-Lee (JWL) EOS for Explosive. In this study, the JWL EOS is used to calculate the pressure induced by detonation products of high explosives. The JWL EOS is expressed as

$$P_J = A_J\left(1 - \frac{\omega}{R_1 V}\right)e^{-R_1 V} + B_J\left(1 - \frac{\omega}{R_2 V}\right)e_1^{-R_2 V} + \frac{\omega E}{V}, \quad (7)$$

where P_J is the pressure of the detonation products, V is the relative volume of detonation products, and E is the special internal energy with initial values of E_0, A_J, B_J, R_1, R_2, and ω that are material constants. The JWL EOS parameters of explosive are listed in Table 2 [43].

2.3. Material Identification of Air. In practice, the radial decoupling charge structure is usually applied in cut blasting to control the damage zone. In this study, the radial air-decoupling charge technique is implemented. Material type 9 of LS-DYNA (∗MAT_NULL) is used to describe the air material by the following EOS:

$$P_A = C_0 + C_1\delta + C_2\delta^2 + C_3\delta^3 + \left(C_4 + C_5\delta + C_6\delta^2\right)e_2, \quad (8)$$

Table 3: Numerical simulation schemes.

Schemes	B (mm)	Φ (mm)	d (mm)	ξ	Air layer (mm)
1	170	250	110	1.737	10
2	220	250	110	1.371	10
3	270	250	110	1.132	10
4	320	250	110	0.964	10
5	370	250	110	0.840	10
6	420	250	110	0.744	10
7	270	220	110	0.989	10
8	270	190	110	0.858	10
9	370	350	110	1.241	10
10	370	450	110	1.723	10
11	370	250	120	0.833	10
12	370	250	130	0.828	10
13	370	250	140	0.827	10

where P_A is the pressure, e_2 is the internal energy per volume, δ is the dynamic viscosity coefficient, and C_0, C_1, C_2, C_3, C_4, C_5, and C_6 are material constants. In this study, the air is assumed to be an ideal gas by setting $C_0 = C_1 = C_2 = C_3 = C_6 = 0$ and $C_4 = C_5 = 0.401$, and air mass density and initial internal energy are 1.255 kg/m^3 and 0.25 J/cm^3, respectively [43].

3. Damage Evolution of Prime Cut Blasting under Different Cut Parameters

The damage evolution process of the prime cut hole blasting can be divided into 4 stages [23]: (1) shock wave induced by explosive acts on the wall of the borehole to produce a compression damage zone around the prime cut hole. (2) With

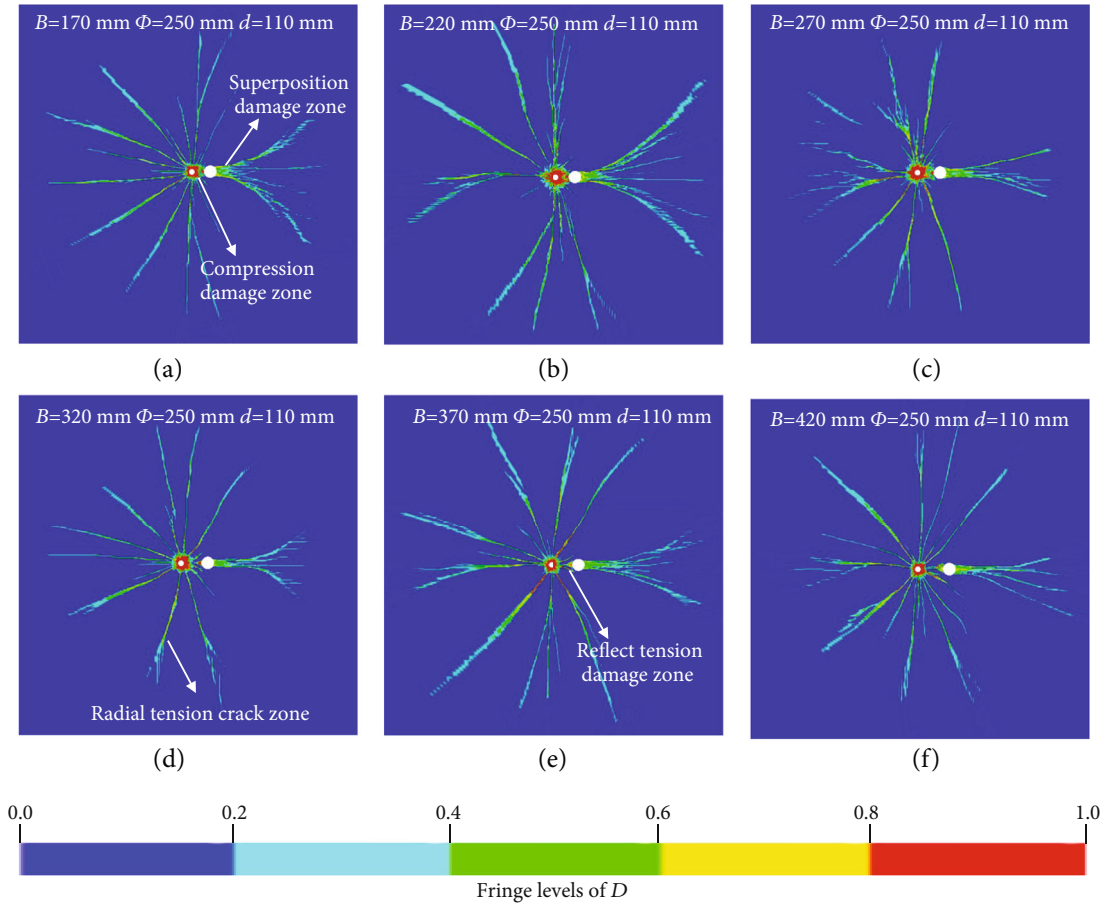

FIGURE 3: Overall damage of prime cut blasting under different burdens: (a) scheme 1, (b) scheme 2, (c) scheme 3, (d) scheme 4, (e) scheme 5, and (f) scheme 6.

the stress wave propagation, a radial tension damage zone appears outside the compression damage zone due to the hoop tensile stress components of stress wave. (3) When the stress wave propagates to the wall of the empty hole, it is reflected to form a tensile wave. The reflection tension damage zone induced by the tensile wave develops to the prime cut hole. Ideally, the reflection tension damage zone and the damage zones surrounding the prime cut hole can be interconnected. (4) The remained stress waves bypass the empty hole and continue to propagate. When the stress wave superposition occurs beyond the empty hole, the tension damage zone initiates within the superposition zone. The ideal result of the prime cut hole blasting is that the burden rock of the prime cut hole is completely damaged and then thrown out from the opening by the static gas pressure. Besides, it is necessary to avoid more radial cracks to extend beyond the cut zone.

3.1. Establishment of the Numerical Model. In this study, LS-DYNA, which is a well-known nonlinear dynamic commercial software, is used to simulate the process of rock damage under burn cut blasting. This software includes Lagrange, Eulerian, and Arbitrary Lagrangian-Eulerian (ALE) algorithm. The process of rock blasting can be regarded as the fluid-structure interaction between the explosive and rock. Thus, the ALE algorithm can be employed to model the fluid-structure interaction characteristic. The explosive and air are modeled with Euler mesh, and the rock material is modeled with Lagrangian mesh in the ALE algorithm. The interaction between explosive and rock is achieved by the keyword "∗CONSTRAINED_LAGRANGE_IN_SOLID."

To study the damage evolution process of the prime cut hole with different cut parameters, a series of numerical simulation schemes are designed based on a simplified cut model which includes a prime cut hole and a large empty hole. The corresponding numerical model, with the dimension of 20 m × 20 m (length×width), is established as shown in Figure 2. An empty hole as a free surface and swelling space is located in the centre of the model, and a prime cut hole is arranged on the left side of the empty hole. The nonreflection boundary conditions are set up in the four outer-rounded sides. The element type is 164 solid element, and the element number is 135240.

The variables of cut parameters consist of length of the burden rock (B) and diameters of the empty hole (Φ) and prime cut hole (d). The scope of the empty hole diameter is not only related to excavation advance but also related

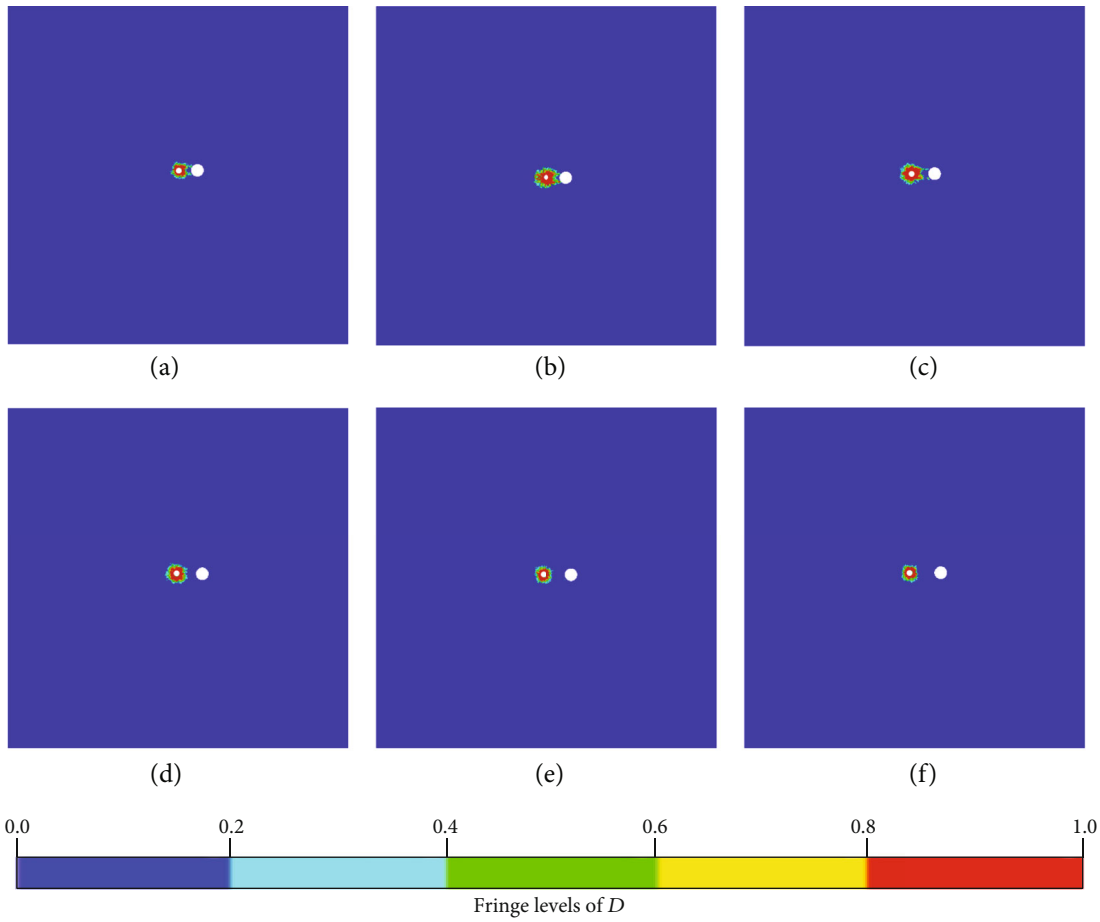

Figure 4: Compression damage of prime cut blasting under different burdens: (a) scheme 1, (b) scheme 2, (c) scheme 3, (d) scheme 4, (e) scheme 5, and (f) scheme 6.

to swelling space. For a deeper raise excavation, it needs larger empty hole. Similarly, for a longer burden, it also needs a larger empty hole. In this study, the depth direction effect is not considered due to the single-element model. Thus, the diameter range of the empty hole is selected based on swelling space. Considering the minimum swelling space for the prime cut hole, the swelling ratio (ζ) of all schemes should be greater than 0.45 [44], as shown in Eq (9).

$$\zeta = \frac{V_s}{V_b} = \frac{2\pi\left(\Phi^2 + d^2\right)}{4B(\Phi + d) + 2(\Phi + d)^2 - \pi\left(\Phi^2 + d^2\right)}, \quad (9)$$

where V_s is the volume of swelling space for the prime cut hole, namely, volume of the empty hole; V_b is the volume of the burden rock; B is the hole spacing between the prime hole and empty hole; Φ and d are the diameter of the empty hole and charge hole, respectively. In order to meet the requirement of the swelling ratio, the value of Φ ranges from 0.19 m to 0.45 m, and B ranges from 0.17 m to 0.42 m. Besides, d ranges from 0.11 m to 0.14 m, which represents the changes of linear charge density. It should note that the thickness of the air layer remains a constant of 10 mm. The scheme design details can be seen from Table 3.

3.2. Analysis of Numerical Simulation Results

3.2.1. Burden for the Prime Cut Hole. The damage evolution results of cut blasting under different burdens are presented in Figure 3. It can be seen that the burden rock is completely damage when the burden is less than or equal to 270 mm. When the burden increases to 320 mm, the burden rock is only partially damage because the compression damage zone and the reflected tension damage zone are not interconnected. Further, compression damage and tension damage are exhibited separately for analysis, as shown in Figures 4 and 5. It can be found from the compression damage results (Figure 4) that the areas of compression damage zones are basically consistent and do not change with the change of burden. The value of the damage variable D is very close to 1, which indicates that the rock in the compression damage zone is completely crushed. The radius of the compression damage zone is about 2~3 times of the diameter of the prime

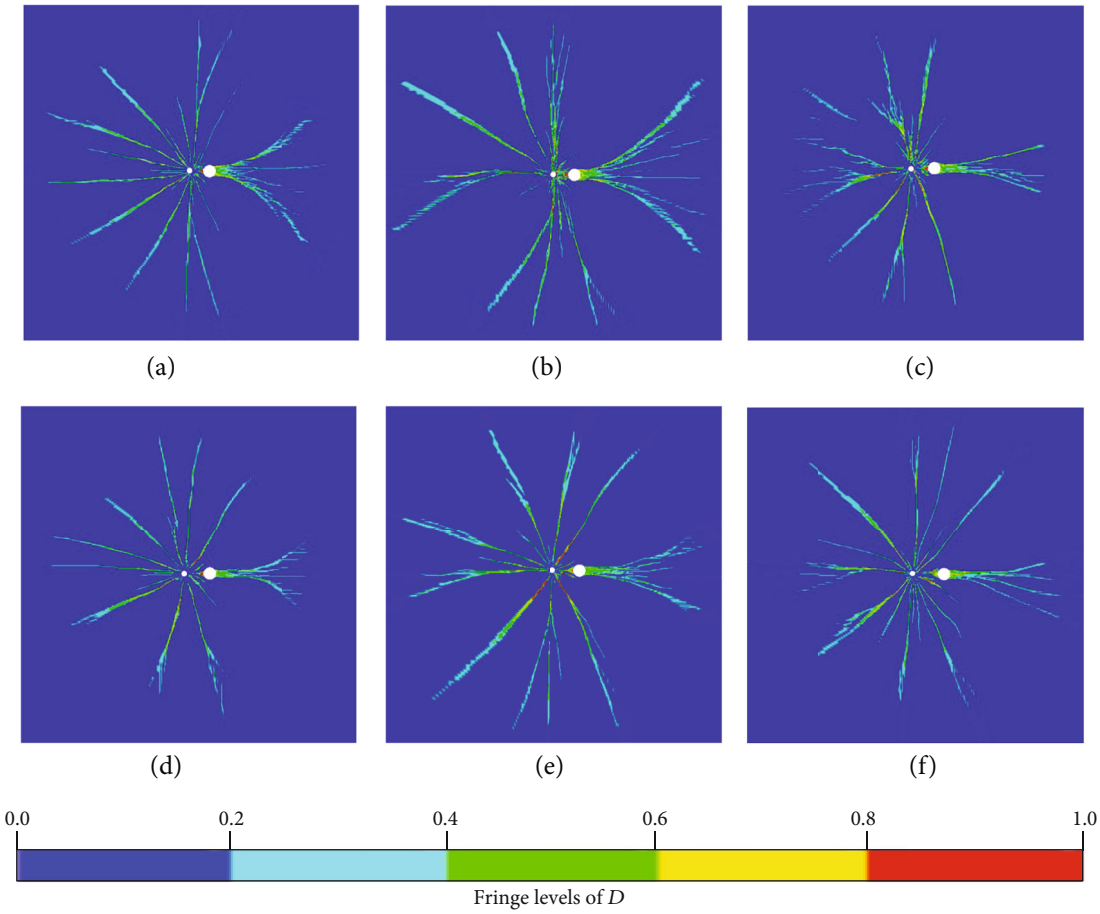

Figure 5: Tension damage of prime cut blasting under different burdens: (a) scheme 1, (b) scheme 2, (c) scheme 3, (d) scheme 4, (e) scheme 5, and (f) scheme 6.

hole, which is consistent with the theoretical calculation value [45], while the reflection tension damage decreases with the increase of the burden. The possible reason is that with the burden increasing, the energy consumed in the process of propagation also increases. When the stress wave propagates to the wall of the empty hole, it has already attenuated greatly, so that the reflected tensile wave induces less damage to the rock.

Further observation can be found in a large number of radial tensile cracks that appear in the direction without an empty hole, as shown in Figure 5. However, there is no large scale radial tensile cracks extending outwards in the direction of the empty hole, most of which are concentrated in the burden rock and the superposition zone behind the empty hole. From the energy point of view, the blasting energy transfers and creates many radial fractures in all directions when a single charge hole initiates in the infinite homogeneous rock mass. However, the blasting energy shifts towards a direction where free surface exists. In the process of cut blasting, the blasting energy shifts towards the empty hole which results in most of the energy being used to break the burden rock in the direction of the empty hole while many radial tensile cracks are formed in other directions. According to the analysis of the simulation results, it can be concluded that the reductions of burden have considerable effect on the improvement of the damage zone, and 270 mm is the suitable burden to maximize the opening in this set of schemes.

3.2.2. Diameter of the Empty Hole. Figure 6 shows the influence of the empty hole diameter (Φ) on damage evolution of the burden rock. Taking schemes 3, 7, and 8 for example, under the burden of 270 mm, the damage zone of the burden rock gradually decreases with the reduce of Φ from 250 mm to 190 mm. Similarly, under the burden of 370 mm, the damage zone of the burden rock for schemes 5, 9, and 10 increases with the increase of Φ from 250 mm to 450 mm, as shown in Figures 6(d)–6(f). In order to study the influence of the empty hole on the development of tension damage, the tension damage evolution is further analyzed individually. It can be found from Figure 7 with the increase of the empty hole diameter, not only the reflected tension damage zone increases, and the radial tensile crack area increases in the direction of the empty hole, while the number and length of radial tensile cracks

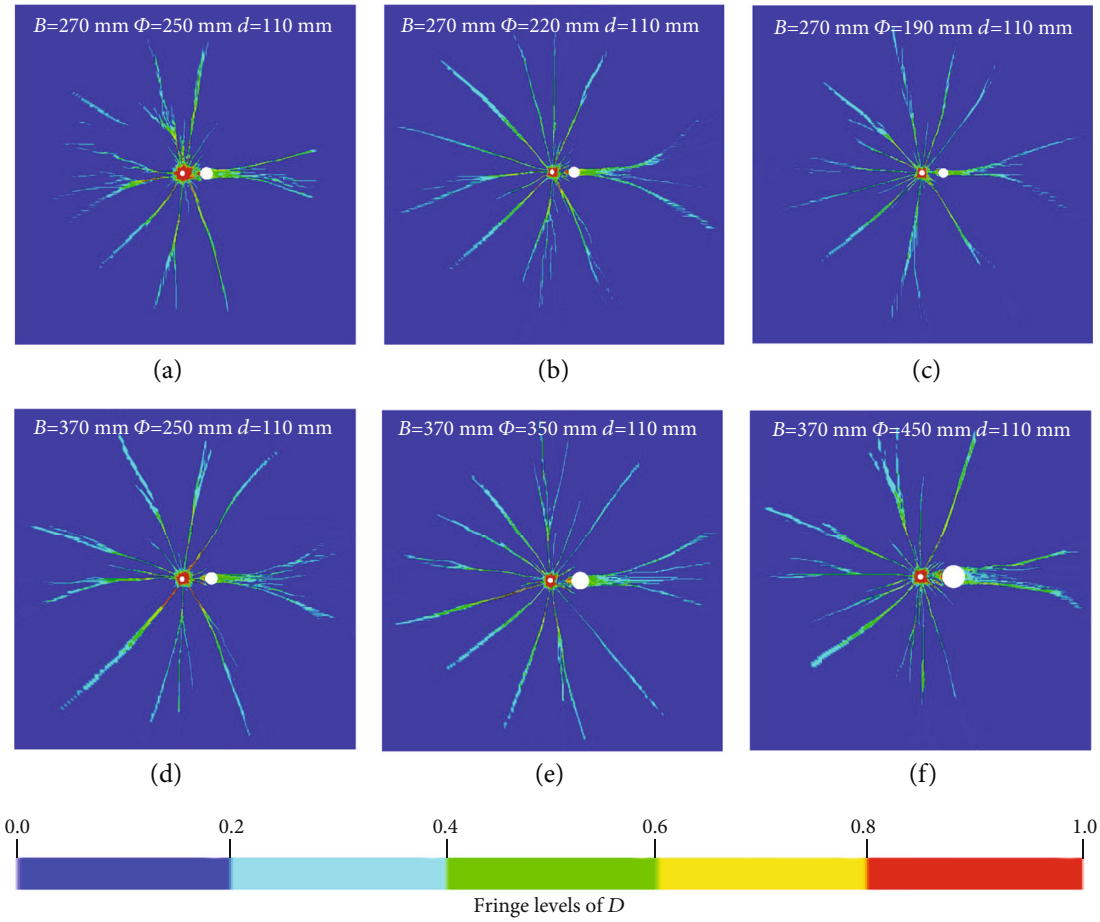

Figure 6: Overall damage of prime cut blasting under different diameters of the empty hole: (a) scheme 3, (b) scheme 7, (c) scheme 8, (d) scheme 5, (e) scheme 9, and (f) scheme 10.

are almost unchanged in other directions in the case of a certain weight of explosive. According to the above analysis, the empty hole has the function of blasting energy shifts. According to the simulation results of the empty hole diameter, it indicates that the size of the empty hole has an important influence on the blasting energy shifts. With the increase of Φ, the tension damage zone increases as well as the reflection tension damage zone in the direction of the empty hole that demonstrates the larger the size of the empty hole, the greater the energy shifts, which is consistent with the observation from Xie et al. [23]. Therefore, the large empty hole is suggested in the burn cut mode, which can not only transfer more explosion energy for the cut zone to break burden rock but also form a larger opening, providing better conditions for the subsequent cut hole blasting.

3.2.3. Diameter of the Prime Cut Hole. The comparisons of the damage zones under different prime cut hole diameters are shown in Figure 8. It can be seen that, with the increase of prime cut hole diameter, the damage zone in the vicinity of the prime cut hole and the radial tensile cracks tend to increase. The main reason is that with the increase of linear charge density, the explosive energy increases. Further, compression damage and tension damage are analyzed separately, as shown in Figures 9 and 10. It can be found that with the increase of linear charge density, the compression damage extends sharply, while the tension damage develops slowly, and only a few short of radial tensile cracks appear in the vicinity of the prime cut hole. It indicates that as the distance to the prime cut hole increases, the consumption of blasting energy decreases. First, most of the blasting energy is consumed in creation of the compression damage zone near the prime cut hole. Then, many radial tensile cracks are increased outside the compression damage zone. Due to the consumption of much blasting energy in the compression damage zone, the length of increased cracks is shorter.

According to the above analysis, there is a threshold of the burden, which can not only maximize the size of cut opening but also avoid incompletely damage of the burden rock. For the empty hole in cut blasting, it can transfer the blasting energy. If the diameter of the empty hole is small, most of the energy will be consumed in the creation of the long radial fractures. If the empty hole is large enough,

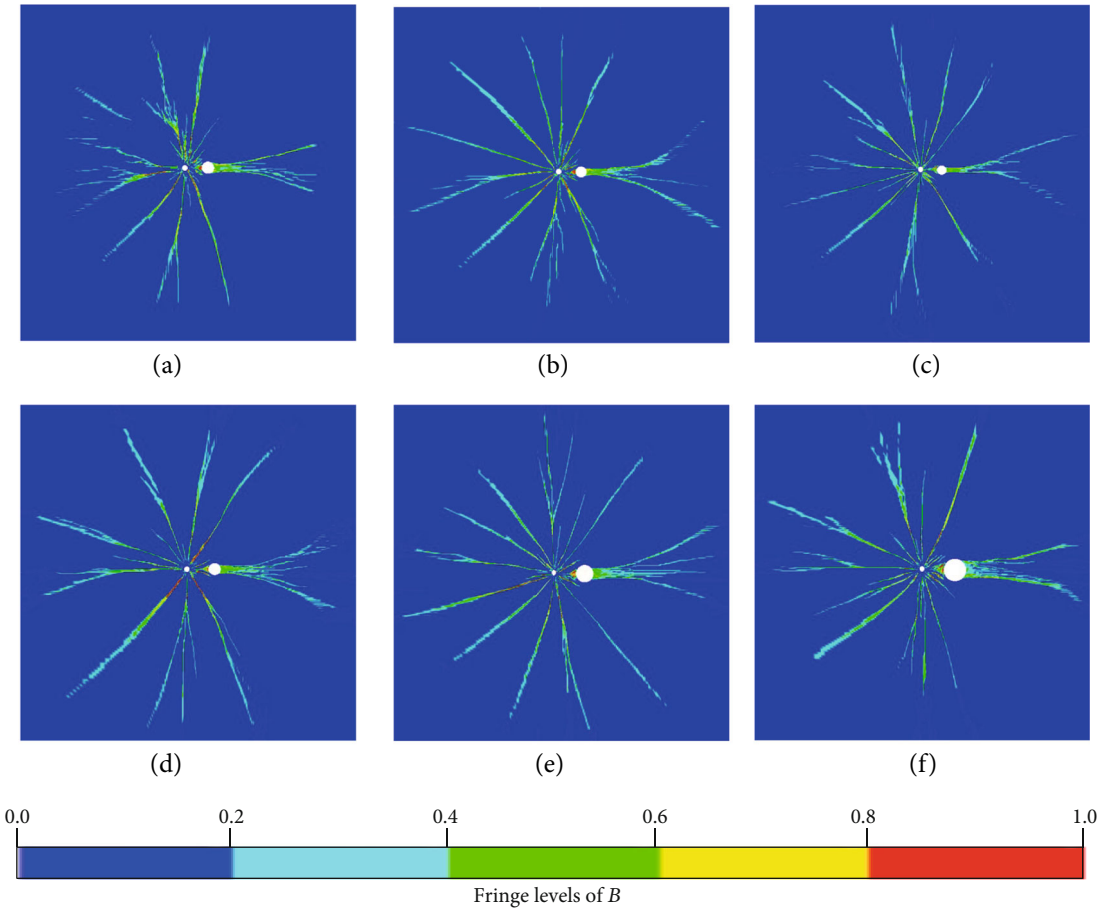

Figure 7: Tension damage of prime cut blasting under different diameters of the empty hole: (a) scheme 3, (b) scheme 7, (c) scheme 8, (d) scheme 5, (e) scheme 9, and (f) scheme 10.

more energy will be shifted in the direction of the empty hole and consumed in the creation of opening. That means that the larger the empty hole the more energy is used in the creation of the opening. However, considering the drilling cost, too large empty hole is waste and not necessary under a certain burden. Further, the increase of line charge density has a direct and obvious effect on rock failure and damage; meanwhile, more long radial cracks will be also created. Therefore, the relationship among the charge hole, burden, and empty hole is that the charge hole provides blasting energy; then, the empty hole transfers the blasting energy to break the burden rock and provides swelling space for rock fragments. In order to obtain a good effect of cut blasting, the relationship of cut parameters should be considered comprehensively.

The prime cut hole initiates to form an opening, which provides a free surface and swelling space for the subsequent cut holes in the process of cut blasting. Thus, appropriate prime cut hole parameters employed in a cut model can ensure the creation of opening. Too many radial cracks induced by improper parameters may influence the results of subsequent cut holes blasting and the stability of wall during one-step raise excavation. In this study, the parameters of $B = 270$ mm, $\Phi = 250$ mm, and $d = 110$ mm (scheme 3) can produce a good effect based on the analysis of numerical results. When the burden increases to 370 mm, it can be also damaged completely under $\Phi = 450$ mm (scheme 10) or $d = 150$ mm (scheme 15). However, the large diameter of the borehole needs high drilling cost. Besides, the increasing of d will lead to much radial fractures that appear.

4. Comparison of the Cut Model Design

In engineering, there are four typical burn cut models for one-step raise excavation [46]: spiral cut, diamond cut, triangular prism cut, and doliform cut, as shown in Figure 11. In this study, the damage evolution processes of cut blasting are investigated to analyze and evaluate the effects of cut blasting under different burn cut models.

The four typical numerical simulation models of burn cut are established, as shown in Figure 11. It can be seen that the optimal cut parameters ($B = 270$ mm, $\Phi = 250$ mm, $d = 110$ mm) obtained from Section 4 are applied in these burn cut models. Figure 11(a) presents the numerical

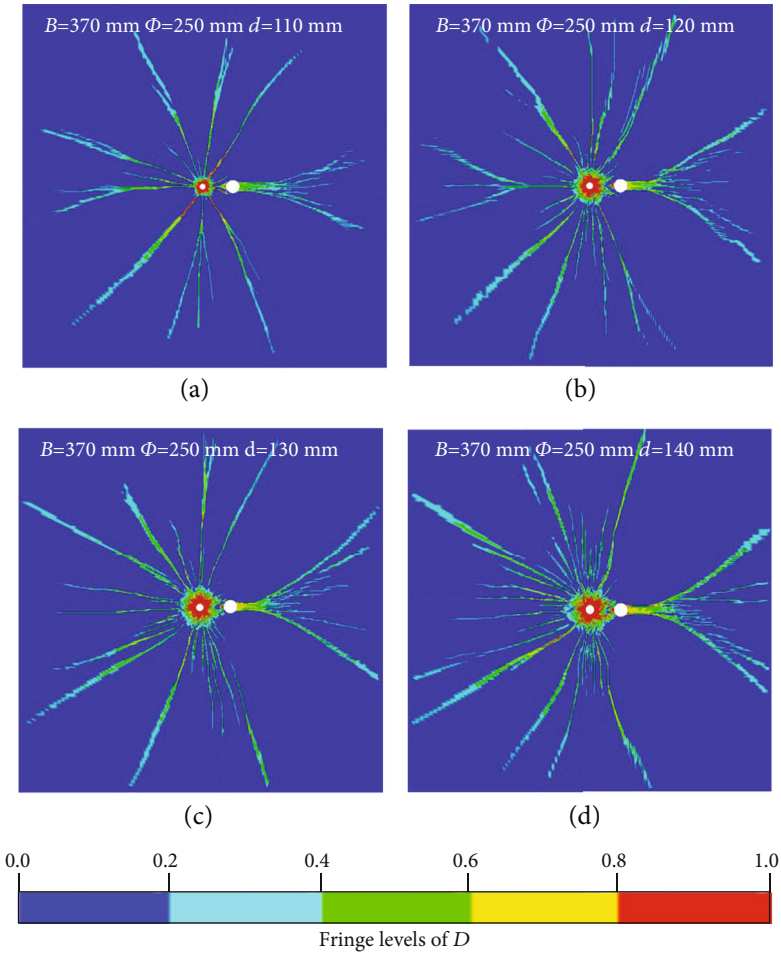

FIGURE 8: Overall damage of prime cut blasting under different diameters of the charge hole: (a) scheme 5, (b) scheme 11, (c) scheme 12, and (d) scheme 13.

model of spiral cut, in which an empty hole is located in the centre of the model, and four cut holes are arranged in spiral around the empty hole. The spiral hole spaces are 0.45 m, 0.5 m, 0.55 m, and 0.7 m, respectively. Seen from Figure 11(b) about diamond cut, two empty holes with 0.2 m distance are created as free surface and swelling space for the prime cut hole, and four cut holes are arranged in diamond around the empty holes. There are three empty holes that are arranged around the prime cut hole in the triangular prism cut as shown in Figure 11(c); then, three secondary cut holes are located in the mid-perpendicular between two adjacent empty holes. The design of the doliform cut, as shown in Figure 11(d), is similar to the triangular prism cut. The boundary conditions and element types of these numerical models with the dimension of $7 \times 7\ m^2$ are kept consistent with the above simplified cut model. In addition, the initiation sequences of the four models are the prime cut hole (0 ms) → second cut hole (2 ms) → third cut hole (4 ms) → fourth cut hole (6 ms). The delay time is set to 2 milliseconds which is less than that in practical engineering due to the effect of gas pressure that is not considered in the numerical simulation.

Figure 12 gives the numerical simulation results of the four types of cut models. It can be seen that the burdens are completely damaged after the detonations in prime cut holes. It clearly demonstrates that the cut parameters are suitable in these cut models. Moreover, it illustrates that more radial fractures extend outward in spiral cut and diamond cut than those in triangular prism cut and doliform cut. The reason for this effect is that with the increase of the empty hole number, the area of the free surface increases; then, more energy shifts towards to the empty holes. Meanwhile, the layout of holes has a significant effect on the development of the damage zone. The empty holes are designed around the prime cut hole in triangular prism cut and doliform cut, in which most energy has been consumed in creation of opening. However, in spiral cut and diamond cut, the empty holes are arranged in one side of the prime cut hole, and the other side is rock mass inducing the formation of radial fractures.

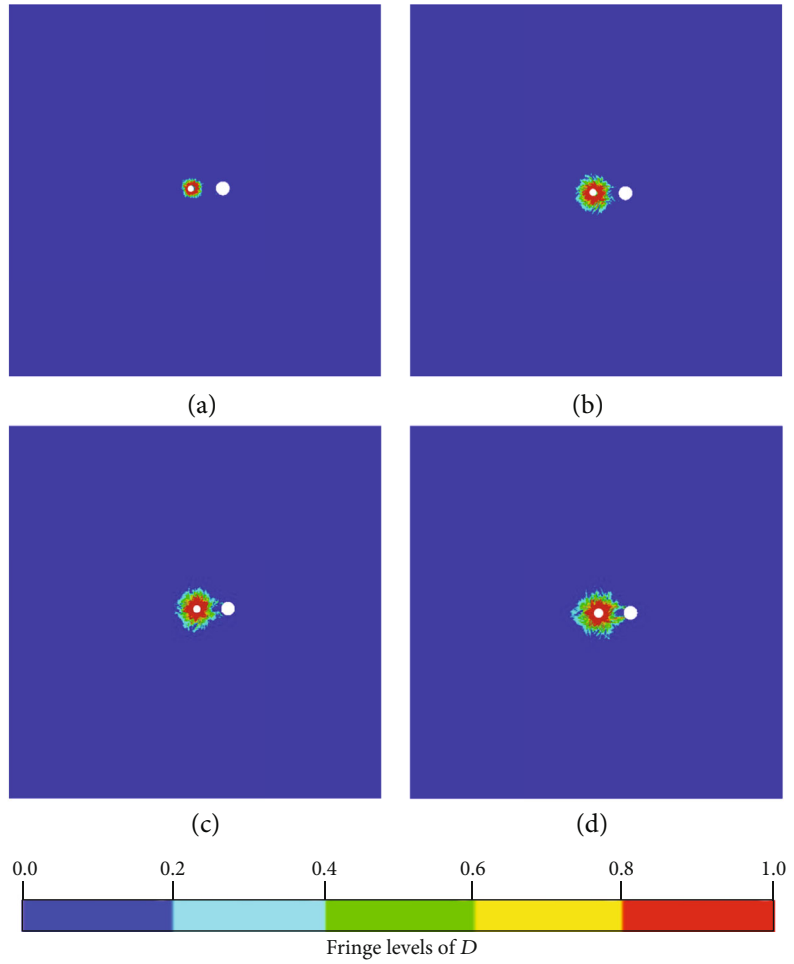

Figure 9: Compression damage of prime cut blasting under different diameters of the charge hole: (a) scheme 5, (b) scheme 11, (c) scheme 12, and (d) scheme 13.

After 2 ms, the secondary cut holes are initiated in sequence, and the corresponding burden rock is completely broken in all numerical models. It can be clearly seen that the processes of cut openings were formed from the four cut models. The length of the radial fractures formed in the previous cut hole blasting greatly increases with the detonation of the next cut hole. Moreover, most of these cracks expanded outside of the cut openings may result in a negative effect for subsequent borehole initiation, even damage of the raise wall. A probable reason is that under the action of new hoop tension stress, the previous formed radial cracks are easy to continue expanding due to the low dynamic tension strength of rock mass.

The numerical results suggest that the number and layout of empty holes have a significant effect on the development of the damage zone. If a burn cut model, which has a few empty holes, is applied in one-step raise excavation, most of the energy will be consumed in creation of long radial cracks. Fortunately, the results will be opposite when the burn cut model has enough empty holes surrounding the prime cut hole. Considering the efficiency and damage control in the one-step raise excavation, the long radial crack should be avoided. So, in order to control the energy used for the creation of the opening, it is necessary to design more empty holes arranged around the prime cut hole in the burn cut model. However, considering the drilling technology and drilling cost, there are many boreholes in the section of triangular prism cut and doliform cut, so the workers' drilling technology requirement is higher, and the drilling cost is also increased accordingly. Therefore, the choice of the burn cut mode is related to the depth of one-step raise excavation. For a deep raise or a blind raise, the burn cut model with more than three empty holes is optimal due to the high degree of constriction of the burden rock. For a raise with a depth of less than 10 m, the burn cut model with single or double empty holes can be adopted to reduce the cost, which is consistent with the research in Ref. [46].

5. Conclusions

In engineering, it is difficult to determine the cut parameters in one-step raise excavation. The objective of this study is to

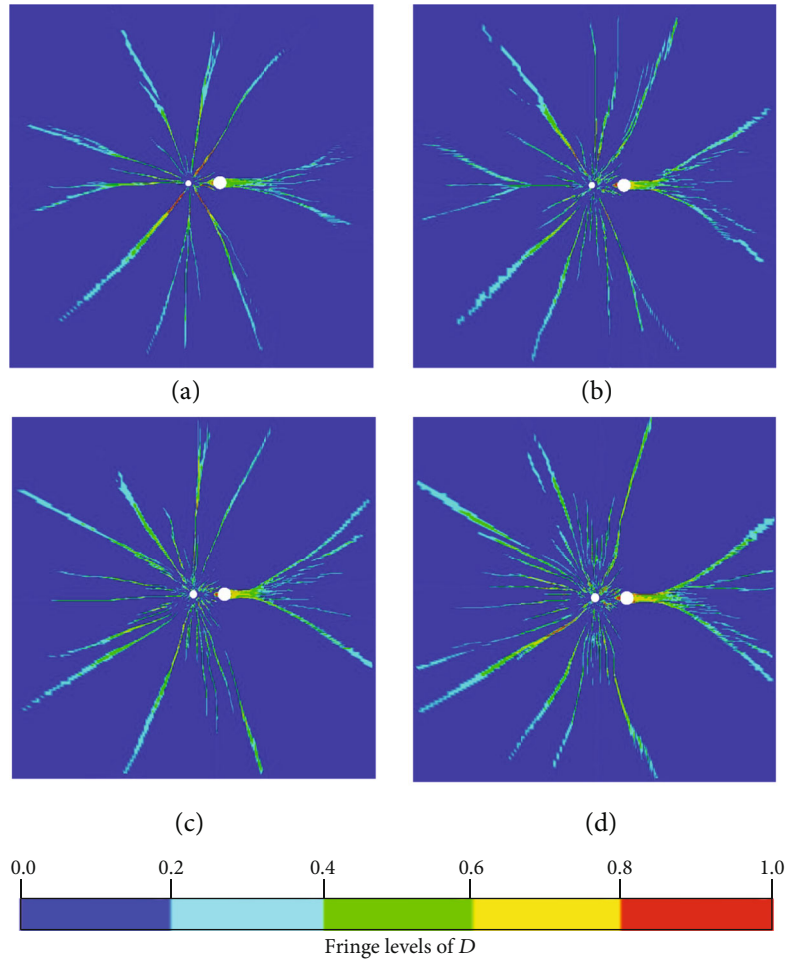

Figure 10: Tension damage of prime cut blasting under different diameters of the charge hole: (a) scheme 5, (b) scheme 11, (c) scheme 12, and (d) scheme 13.

analyze the relationship between cut parameters and damage zones by using the numerical simulation method. Further, to achieve the optimal cut parameters, which are applied on four typical burn cut models to recommend a reasonable cut model by comparing the damage evolution and blasting energy utilization, the main conclusions can be drawn as follows:

(1) The ideal burden length can maximize the use of blasting energy. When the burden is lower than the ideal value, only part of the energy is consumed in the creation of opening while the excess energy is wasted in the creation of long radial cracks. When the burden is greater than the ideal value, the burden rock may be incompletely damaged leading to the result that the opening cannot be formed

(2) The empty hole as a free surface is effective in controlling the size and develop direction of the damage zone. With the increase of the empty hole diameter, more and more energy will be shift towards to the empty hole and consumed in the creation of opening. It demonstrates that the advantage of the large empty hole in burn cut

(3) The linear charge density of the prime cut hole has a significant effect on damage evolution of cut blasting. The increase of the linear charge density means the increase of explosive energy, which will lead to the increase of the entire damage zone including burden damage and radial fractures. The optimal way to control most energy consumed in burden is that the diameter of the empty hole increases with the increase of the linear charge density

(4) For spiral cut and diamond cut, there are only a few empty holes that are arranged in one side of the prime cut hole, and much blasting energy that is wasted results in that long radial fractures that are created in the other directions without an empty hole. For triangular prism cut and doliform cut, in which the layout of empty holes surrounds the prime cut

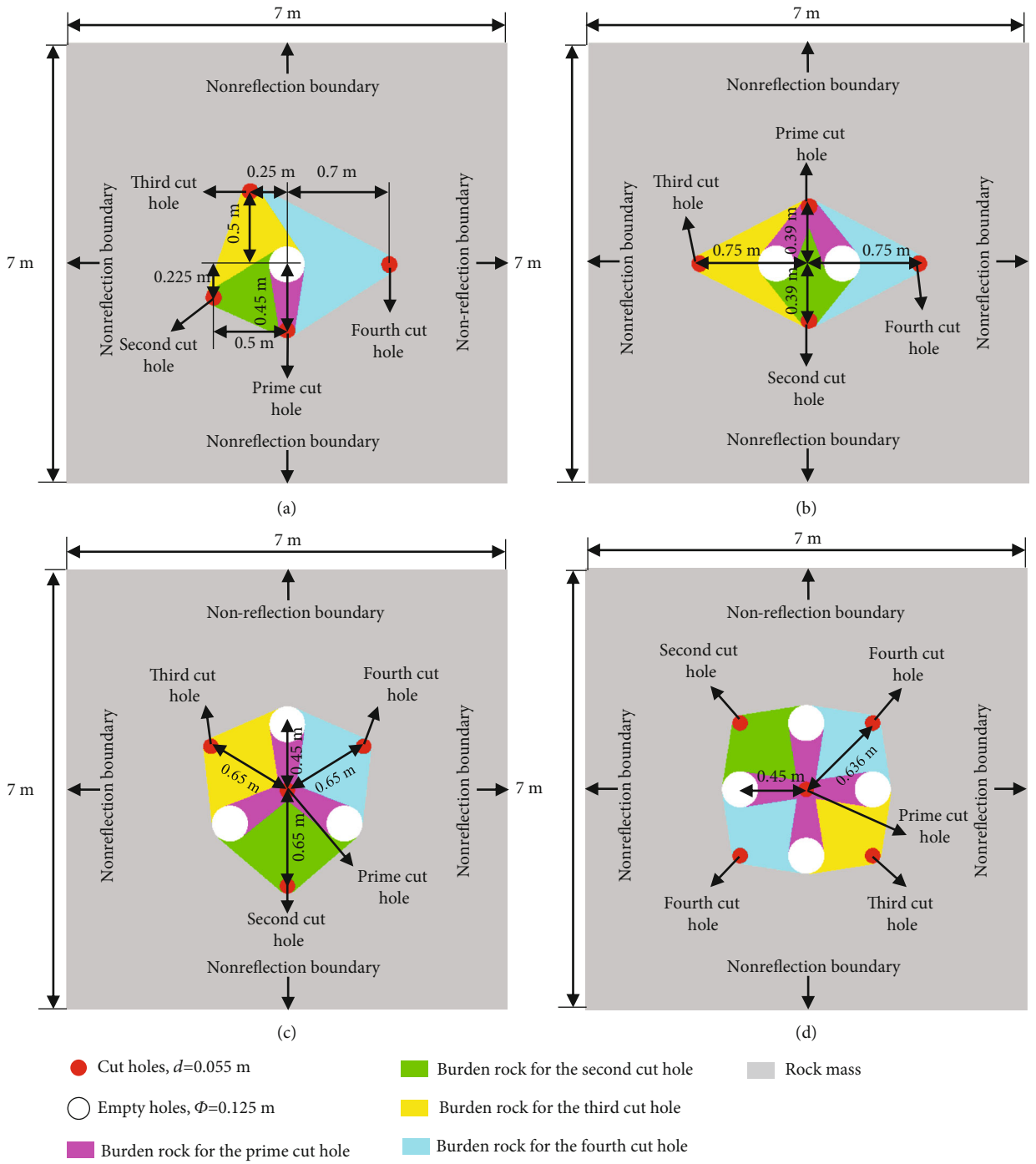

Figure 11: Four types of burn cut models with geometry and boundary conditions: (a) spiral cut, (b) diamond cut, (c) triangular prism cut, and (d) doliform cut.

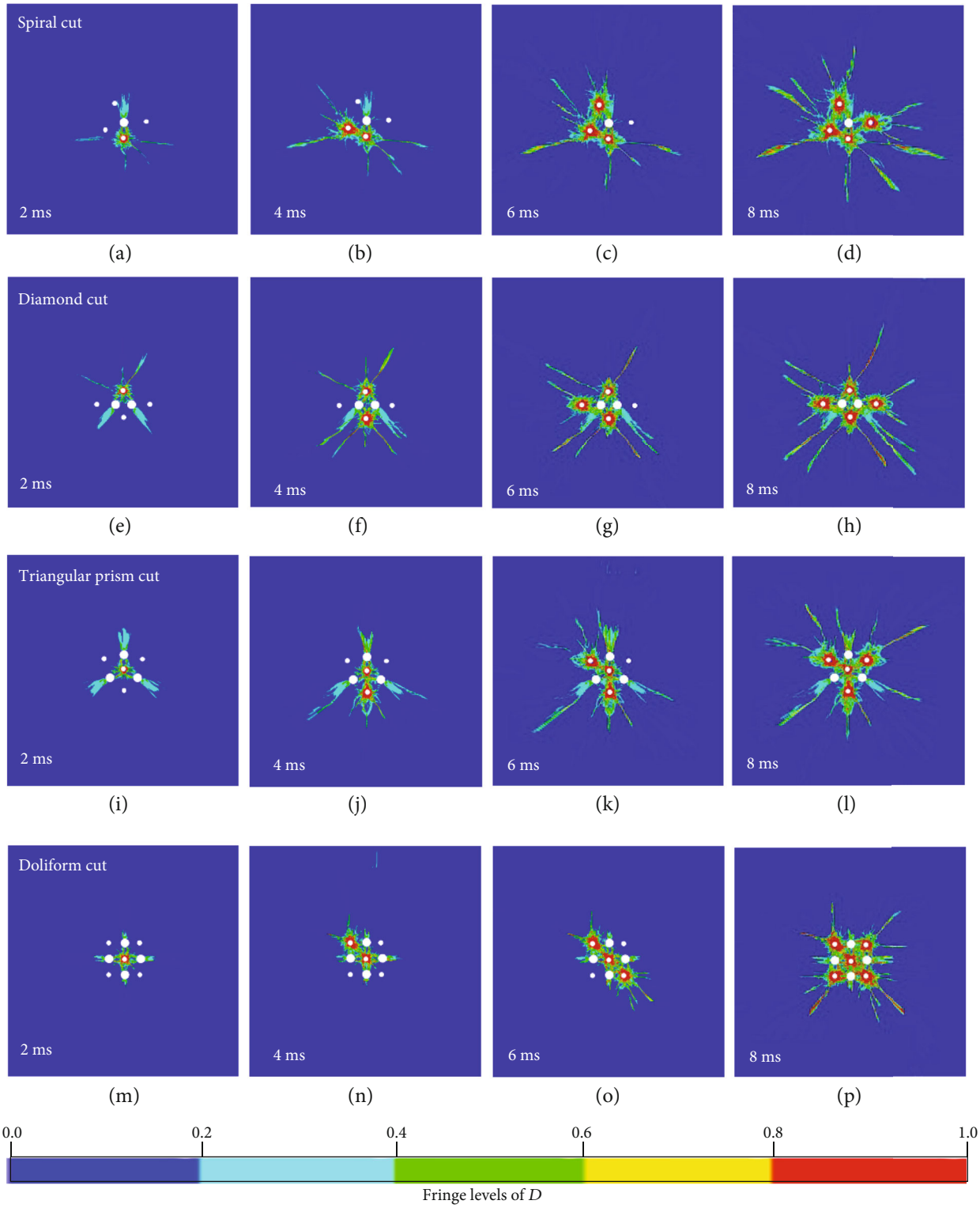

Figure 12: Cut blasting processes of four burn cut models: (a)–(d) spiral cut blasting process, (e)–(h) diamond cut blasting process, (i)–(l) triangular prism cut blasting process, and (m)–(p) doliform cut blasting process.

hole, the corresponding burdens are damaged completely, and few radial fractures appear

Data Availability

All data, models, and code generated or used during the study can be found from the relevant references or appear in the submitted article.

Conflicts of Interest

The authors declare no conflict of interest.

Acknowledgments

The authors gratefully acknowledge the financial support of the China Postdoctoral Science Foundation (2019M662840), the National Key Research and Development Program of China (2016YFC0600706 and 2016YFC0600802) and Funded by the Open Research Fund Program of Key Laboratory of Metallogenic Prediction of Nonferrous Metals and Geological Environment Monitoring (Central South University), Ministry of Education (2020YSJS13).

References

[1] S. Zare and A. Bruland, "Comparison of tunnel blast design models," *Tunnelling and Underground Space Technology*, vol. 21, no. 5, pp. 533–541, 2006.

[2] Z. Zhao, Y. Zhang, and H. Bao, "Tunnel blasting simulations by the discontinuous deformation analysis," *International Journal of Computational Methods*, vol. 8, no. 2, pp. 277–292, 2011.

[3] H. Hao, C. Q. Wu, and Y. Zhou, "Numerical analysis of blast-induced stress waves in a rock mass with anisotropic continuum damage models part 1: equivalent material property approach," *Rock Mechanics and Rock Engineering*, vol. 35, no. 2, pp. 79–94, 2002.

[4] H. Hao, C. Q. Wu, and Y. Zhou, "Numerical analysis of blast-induced stress waves in a rock mass with anisotropic continuum damage models part 2: stochastic approach," *Rock Mechanics and Rock Engineering*, vol. 35, no. 2, pp. 95–108, 2002.

[5] J. H. Shin, H. G. Moon, and S. E. Chea, "Effect of blast-induced vibration on existing tunnels in soft rocks," *Tunnelling and Underground Space Technology*, vol. 26, no. 1, pp. 51–61, 2011.

[6] J. D. Qiu, D. Li, X. Li, and Q. Zhu, "Numerical investigation on the stress evolution and failure behavior for deep roadway under blasting disturbance," *Soil Dynamics and Earthquake Engineering*, vol. 137, p. 106278, 2020.

[7] Q. Y. Li, K. Liu, X. B. Li, Z. W. Wang, and L. Weng, "Cutting parameter optimization for one-step shaft excavation technique based on parallel cutting method," *Transactions of Nonferrous Metals Society of China*, vol. 28, no. 7, pp. 1413–1423, 2018.

[8] L. M. Taylor, E. P. Chen, and J. S. Kuszmaul, "Microcrack-induced damage accumulation in brittle rock under dynamic loading," *Computer Methods in Applied Mechanics and Engineering*, vol. 55, no. 3, pp. 301–320, 1986.

[9] G. R. Johnson and T. J. Holmquist, "A computational constitutive model for brittle materials subjected to large strains, high strain rates and high pressures," in *Shock Wave and High-Strain-Rate Phenomena in Materials*, pp. 1075–1081, CRC Press, Boca Raton, FL, USA, 1992.

[10] W. Riedel, K. Thoma, S. Hiermaier, and E. Schmolinske, "Penetration of reinforced concrete by BETA-B-500 numerical analysis using a new macroscopic concrete model for hydrocedes," in *Proceedings of the 9th International Symposium on the Effects of Munitions with Structures*, Berlin, Germany, 1999.

[11] Z. L. Wang, Y. C. Li, and R. F. Shen, "Numerical simulation of tensile damage and blast crater in brittle rock due to underground explosion," *International Journal of Rock Mechanics and Mining Sciences*, vol. 44, no. 5, pp. 730–738, 2007.

[12] Q. Fang, X. Kong, H. Wu, and Z. Gong, "Determination of Holmquist-Johnson-cook consitiutive model parameters of rock," *Engineering Mechanics*, vol. 31, no. 3, pp. 197–204, 2014.

[13] K. Liu, Q. Y. Li, C. Q. Wu, X. B. Li, and J. Li, "A study of cut blasting for one-step raise excavation based on numerical simulation and field blast tests," *International Journal of Rock Mechanics and Mining Sciences*, vol. 109, pp. 91–104, 2018.

[14] M. M. Shahzamanian, "Implementation of a rate dependent tensile failure model for brittle materials in ABAQUS," *International Journal of Impact Engineering*, vol. 97, pp. 127–147, 2016.

[15] M. Polanco-Loria, O. S. Hopperstad, T. Børvik, and T. Berstad, "Numerical predictions of ballistic limits for concrete slabs using a modified version of the HJC concrete model," *International Journal of Impact Engineering*, vol. 35, no. 5, pp. 290–303, 2008.

[16] R. M. Brannon and S. Leelavanichkul, "Survey of four damage models for concrete. Sandia report, Sand 2009-5544," in *Prepared by Sandia National Laboratories*, pp. 1–82, Sandia Laboratory, California, USA, 2009.

[17] C. Yi, J. Sjöberg, and D. Johansson, "Numerical modelling for blast-induced fragmentation in sublevel caving mines," *Tunnelling and Underground Space Technology*, vol. 68, pp. 167–173, 2017.

[18] Y. Q. Zhang, H. Hao, and Y. Lu, "Anisotropic dynamic damage and fragmentation of rock materials under explosive loading," *International Journal of Engineering Science*, vol. 41, no. 9, pp. 917–929, 2003.

[19] S. Xie, H. Lin, Y. Wang et al., "A statistical damage constitutive model considering whole joint shear deformation," *International Journal of Damage Mechanics*, vol. 29, no. 6, pp. 988–1008, 2020.

[20] H. Lin, X. Zhang, Y. X. Wang et al., "Improved nonlinear Nishihara shear creep model with variable parameters for rock-like materials," *Advances in Civil Engineering*, Article ID 7302141, 15 pages, 2020.

[21] L. Liu and P. D. Katsabanis, "Development of a continuum damage model for blasting analysis," *International Journal of Rock Mechanics and Mining Sciences*, vol. 34, no. 2, pp. 217–231, 1997.

[22] Z. Tu and Y. Lu, "Modifications of RHT material model for improved numerical simulation of dynamic response of concrete," *International Journal of Impact Engineering*, vol. 37, no. 10, pp. 1072–1082, 2010.

[23] L. X. Xie, W. B. Lu, Q. B. Zhang, Q. H. Jiang, M. Chen, and J. Zhao, "Analysis of damage mechanisms and optimization

of cut blasting design under high in-situ stresses," *Tunnelling and Underground Space Technology*, vol. 66, pp. 19–33, 2017.

[24] Z. X. Zhang, "Rock blasting in open cut and tunneling," in *Rock Fracture and Blasting*, p. 528, 2016.

[25] K. Liu, C. Wu, X. Li, Q. Li, J. Fang, and J. Liu, "A modified HJC model for improved dynamic response of brittle materials under blasting loads," *Computers and Geotechnics*, vol. 123, p. 103584, 2020.

[26] H. K. Kutter and C. Fairhurst, "On the fracture process in blasting. International journal of rock mechanics and mining sciences & Geomechanics abstracts," *Pergamon*, vol. 8, no. 3, pp. 181–202, 1971.

[27] O. Yilmaz and T. Unlu, "Three dimensional numerical rock damage analysis under blasting load," *Tunnelling and Underground Space Technology*, vol. 38, pp. 266–278, 2013.

[28] S. H. Cho and K. Kaneko, "Influence of the applied pressure waveform on the dynamic fracture processes in rock," *International Journal of Rock Mechanics and Mining Sciences*, vol. 41, no. 5, pp. 771–784, 2004.

[29] G. W. Ma and X. M. An, "Numerical simulation of blasting-induced rock fractures," *International Journal of Rock Mechanics and Mining Sciences*, vol. 45, no. 6, pp. 966–975, 2008.

[30] L. X. Xie, W. B. Lu, Q. B. Zhang, Q. H. Jiang, G. H. Wang, and J. Zhao, "Damage evolution mechanisms of rock in deep tunnels induced by cut blasting," *Tunnelling and Underground Space Technology*, vol. 58, pp. 257–270, 2016.

[31] J. D. Qiu, X. B. Li, D. Y. Li, Y. Z. Zhao, C. W. Hu, and L. S. Liang, "Physical model test on the deformation behavior of an underground tunnel under blasting disturbance," *Rock Mechanics and Rock Engineering*, 2020.

[32] C. L. Wang, Y. Zhao, Y. L. Zhao, and W. Wan, "Study on the interaction of collinear cracks and wing cracks and cracking behavior of rock under uniaxial compression," *Advances in Civil Engineering*, vol. 2018, Article ID 5459307, 10 pages, 2018.

[33] Y. Zhao, P. F. He, Y. F. Zhang, and C. L. Wang, "A new criterion for a toughness-dominated hydraulic fracture crossing a natural frictional interface," *Rock Mechanics and Rock Engineering*, vol. 52, no. 8, pp. 2617–2629, 2019.

[34] Y. L. Zhao, Y. X. Wang, W. Wang, L. Tang, Q. Liu, and G. Cheng, "Modeling of rheological fracture behavior of rock cracks subjected to hydraulic pressure and far field stresses," *Theoretical and Applied Fracture Mechanics*, vol. 101, pp. 59–66, 2019.

[35] Q. H. Wu, L. Weng, Y. L. Zhao, F. J. Zhao, W. Q. Peng, and S. P. Zhang, "Deformation and cracking characteristics of ring-shaped granite with inclusion under diametrical compression," *Arabian Journal of Geosciences*, vol. 13, no. 14, p. 681, 2020.

[36] M. D. Wei, F. Dai, N. W. Xu, T. Zhao, and K. W. Xia, "Experimental and numerical study on the fracture process zone and fracture toughness determination for ISRM-suggested semi-circular bend rock specimen," *Engineering Fracture Mechanics*, vol. 154, pp. 43–56, 2016.

[37] M. D. Wei, F. Dai, N. W. Xu, T. Zhao, and Y. Liu, "An experimental and theoretical assessment of semi-circular bend specimens with chevron and straight-through notches for mode I fracture toughness testing of rocks," *International Journal of Rock Mechanics and Mining Sciences*, vol. 99, pp. 28–38, 2017.

[38] Q. H. Wu, X. B. Li, L. Weng, Q. F. Li, Y. J. Zhu, and R. Luo, "Experimental investigation of the dynamic response of pre-stressed rockbolt by using an SHPB-based rockbolt test system," *unnelling and Underground Space Technology*, vol. 93, p. 103088, 2019.

[39] C. Z. Qi and Q. H. Qian, "Physical mechanism of dependence of material strength on strain rate for rock-like material," *Chinese Journal of Rock Mechanics and Engineering*, vol. 22, no. 2, pp. 177–181, 2003.

[40] Z. R. Wang and Z. H. Zhang, "On the physical significance of the third invariant of stress deviator J3 and the third invariant of stress tensor I3 and their geometric significance in the space of principle stresses," *Journal of Harbin institute of technology*, vol. 2, pp. 108–113, 1982.

[41] J. W. Tedesco, J. C. Powell, C. A. Ross, and M. L. Hughes, "A strain-rate-dependent concrete material model for ADINA," *Computers and Structures*, vol. 64, no. 5-6, pp. 1053–1067, 1997.

[42] J. Weerheijm and J. C. A. M. van Doormaal, "Tensile failure of concrete at high loading rates: new test data on strength and fracture energy from instrumented spalling tests," *International Journal of Impact Engineering*, vol. 34, no. 3, pp. 609–626, 2007.

[43] K. Liu, Q. Y. Li, C. Q. Wu, X. B. Li, and J. Li, "Optimization of spherical cartridge blasting mode in one-step raise excavation using pre-split blasting," *International Journal of Rock Mechanics and Mining Sciences*, vol. 126, p. 104182, 2020.

[44] Q. Liu and H. Tran, "Drilling and Blasting Techniques for Developing Inverse Drop Raises," in *Proceedings of sixth international symposium on rock fragmentation by blasting*, Johannesburg, South Africa, 1999.

[45] J. Dai, "Calculation of radii of the broken and cracked areas in rock by a long charge explosion," *Journal of Liaoning Technical University (Natural Science)*, vol. 20, no. 2, pp. 144–147, 2001, (in Chinese).

[46] Q. Y. Li, X. B. Li, Z. P. Fan, and R. H. Zhang, "One time deep hole raise blasting technology and case study," *Chinese Journal of Rock Mechanics and Engineering*, vol. 32, no. 4, pp. 664–670, 2013.